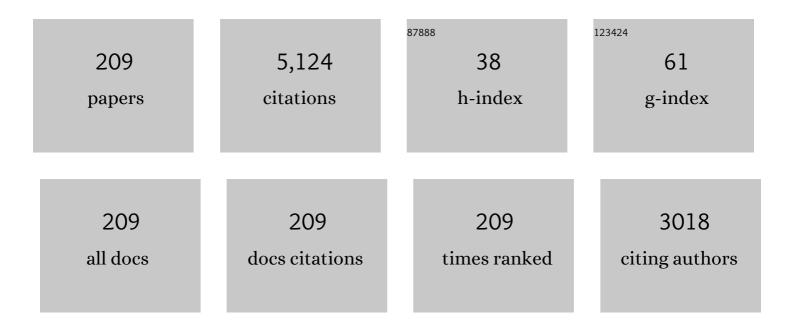
Tomy Varghese

List of Publications by Year in descending order

Source: https://exaly.com/author-pdf/8760400/publications.pdf

Version: 2024-02-01



#	Article	IF	CITATIONS
1	Elastography: Imaging the elastic properties of soft tissues with ultrasound. Journal of Medical Ultrasonics (2001), 2002, 29, 155-171.	1.3	286
2	Tissue-mimicking agar/gelatin materials for use in heterogeneous elastography phantoms. Physics in Medicine and Biology, 2005, 50, 5597-5618.	3.0	242
3	An analysis of elastographic contrast-to-noise ratio. Ultrasound in Medicine and Biology, 1998, 24, 915-924.	1.5	148
4	Viscoelastic characterization ofin vitrocanine tissue. Physics in Medicine and Biology, 2004, 49, 4207-4218.	3.0	146
5	Quasi-Static Ultrasound Elastography. Ultrasound Clinics, 2009, 4, 323-338.	0.2	143
6	Two-dimensional multi-level strain estimation for discontinuous tissue. Physics in Medicine and Biology, 2007, 52, 389-401.	3.0	134
7	Transrectal quantitative shear wave elastography in the detection and characterisation of prostate cancer. Surgical Endoscopy and Other Interventional Techniques, 2013, 27, 3280-3287.	2.4	95
8	Anthropomorphic breast phantoms for testing elastography systems. Ultrasound in Medicine and Biology, 2006, 32, 857-874.	1.5	92
9	Preliminary <i>in vivo</i> atherosclerotic carotid plaque characterization using the accumulated axial strain and relative lateral shift strain indices. Physics in Medicine and Biology, 2008, 53, 6377-6394.	3.0	92
10	Meanâ€scatterer spacing estimates with spectral correlation. Journal of the Acoustical Society of America, 1994, 96, 3504-3515.	1.1	85
11	Elastographic Measurement of the Area and Volume of Thermal Lesions Resulting from Radiofrequency Ablation: Pathologic Correlation. American Journal of Roentgenology, 2003, 181, 701-707.	2.2	84
12	Monitoring stiffness changes in lesions after radiofrequency ablation at different temperatures and durations of ablation. Ultrasound in Medicine and Biology, 2005, 31, 415-422.	1.5	78
13	Hybrid Spectral Domain Method for Attenuation Slope Estimation. Ultrasound in Medicine and Biology, 2008, 34, 1808-1819.	1.5	77
14	Elastography: A systems approach. International Journal of Imaging Systems and Technology, 1997, 8, 89-103.	4.1	76
15	A Review of Carotid Atherosclerosis and Vascular Cognitive Decline. Neurosurgery, 2010, 67, 484-494.	1.1	76
16	Attenuation estimation using spectral cross-correlation. IEEE Transactions on Ultrasonics, Ferroelectrics, and Frequency Control, 2007, 54, 510-519.	3.0	69
17	Stability of heterogeneous elastography phantoms made from oil dispersions in aqueous gels. Ultrasound in Medicine and Biology, 2006, 32, 261-270.	1.5	66
18	Improvement of elastographic displacement estimation using a two-step cross-correlation method. Ultrasound in Medicine and Biology, 2007, 33, 48-56.	1.5	65

#	Article	IF	CITATIONS
19	Performance Optimization in Elastography: Multicompression with Temporal Stretching. Ultrasonic Imaging, 1996, 18, 193-214.	2.6	64
20	Characterization of Elastographic Noise Using the Envelope of Echo Signals. Ultrasound in Medicine and Biology, 1998, 24, 543-555.	1.5	62
21	Histopathologic Validation of Grayscale Carotid Plaque Characteristics Related to Plaque Vulnerability. Ultrasound in Medicine and Biology, 2017, 43, 129-137.	1.5	58
22	Normal and shear strain estimation using beam steering on linear-array transducers. Ultrasound in Medicine and Biology, 2007, 33, 57-66.	1.5	57
23	Frequency-dependent complex modulus of the uterus: preliminary results. Physics in Medicine and Biology, 2006, 51, 3683-3695.	3.0	56
24	Theoretical Bounds on the Estimation of Transverse Displacement, Transverse Strain and Poisson's Ratio in Elastography. Ultrasonic Imaging, 2000, 22, 153-177.	2.6	55
25	Measurement of tendon strain during muscle twitch contractions using ultrasound elastography. IEEE Transactions on Ultrasonics, Ferroelectrics, and Frequency Control, 2009, 56, 27-35.	3.0	55
26	Ultrasonic Imaging of Myocardial Strain Using Cardiac Elastography. Ultrasonic Imaging, 2003, 25, 1-16.	2.6	54
27	Carotid atherosclerotic plaque instability and cognition determined by ultrasound-measured plaque strain in asymptomatic patients with significant stenosis. Journal of Neurosurgery, 2018, 128, 111-119.	1.6	54
28	Bayesian Regularization Applied to Ultrasound Strain Imaging. IEEE Transactions on Biomedical Engineering, 2011, 58, 1612-1620.	4.2	53
29	The nonstationary strain filter in elastography: Part I. Frequency dependent attenuation. Ultrasound in Medicine and Biology, 1997, 23, 1343-1356.	1.5	52
30	Three-Dimensional Electrode Displacement Elastography Using the Siemens C7F2 fourSight Four-Dimensional Ultrasound Transducer. Ultrasound in Medicine and Biology, 2008, 34, 1307-1316.	1.5	52
31	Statistics of ultrasonic scatterer size estimation with a reference phantom. Journal of the Acoustical Society of America, 2003, 113, 3430.	1.1	47
32	Investigation of temperature-dependent viscoelastic properties of thermal lesions in ex vivo animal liver tissue. Journal of Biomechanics, 2009, 42, 959-966.	2.1	46
33	Axial-Shear Strain Imaging for Differentiating Benign and Malignant Breast Masses. Ultrasound in Medicine and Biology, 2010, 36, 1813-1824.	1.5	45
34	Elastographic Dynamic Range Expansion Using Variable Applied Strains. Ultrasonic Imaging, 1997, 19, 145-166.	2.6	43
35	Impact of Gas Bubbles Generated During Interstitial Ablation on Elastographic Depiction of In Vitro Thermal Lesions. Journal of Ultrasound in Medicine, 2004, 23, 535-544.	1.7	41
36	Wavelet denoising of displacement estimates in elastography. Ultrasound in Medicine and Biology, 2004, 30, 477-491.	1.5	40

#	Article	IF	CITATIONS
37	Young's Modulus Reconstruction for Radio-Frequency Ablation Electrode-Induced Displacement Fields: A Feasibility Study. IEEE Transactions on Medical Imaging, 2009, 28, 1325-1334.	8.9	40
38	Correlation of Cognitive Function with Ultrasound Strain Indices in Carotid Plaque. Ultrasound in Medicine and Biology, 2014, 40, 78-89.	1.5	40
39	Spatial Angular Compounding for Elastography without the Incompressibility Assumption. Ultrasonic Imaging, 2005, 27, 256-270.	2.6	38
40	The ultrasonix 500RP: A commercial ultrasound research interface. IEEE Transactions on Ultrasonics, Ferroelectrics, and Frequency Control, 2006, 53, 1772-1782.	3.0	38
41	Classification of Symptomatic and Asymptomatic Patients with and without Cognitive Decline Using Non-invasive Carotid Plaque Strain Indices as Biomarkers. Ultrasound in Medicine and Biology, 2016, 42, 909-918.	1.5	38
42	Elastographic Imaging of Thermal Lesions in Liver <i>In-Vivo</i> Using Diaphragmatic Stimuli. Ultrasonic Imaging, 2004, 26, 18-28.	2.6	36
43	Radioâ€frequency ablation electrode displacement elastography: A phantom study. Medical Physics, 2008, 35, 2432-2442.	3.0	36
44	Estimating tissue strain from signal decorrelation using the correlation coefficient. Ultrasound in Medicine and Biology, 1996, 22, 1249-1254.	1.5	35
45	Improvements in elastographic contrast-to-noise ratio using spatial-angular compounding. Ultrasound in Medicine and Biology, 2005, 31, 529-536.	1.5	35
46	Comparison of cardiac displacement and strain imaging using ultrasound radiofrequency and envelope signals. Ultrasonics, 2013, 53, 782-792.	3.9	35
47	Characterization of Tissue Microstructure Scatterer Distribution with Spectral Correlation. Ultrasonic Imaging, 1993, 15, 238-254.	2.6	33
48	Spherical lesion phantoms for testing the performance of elastography systems. Physics in Medicine and Biology, 2005, 50, 5983-5995.	3.0	33
49	Initial Clinical Experience Imaging Scatterer Size and Strain in Thyroid Nodules. Journal of Ultrasound in Medicine, 2006, 25, 1021-1029.	1.7	33
50	Electrode displacement strain imaging of thermallyâ€∎blated liver tissue in an <i>in vivo</i> animal model. Medical Physics, 2010, 37, 1075-1082.	3.0	33
51	Spatial-angular compounding for elastography using beam steering on linear array transducers. Medical Physics, 2006, 33, 618-626.	3.0	32
52	Shear Wave Velocity Imaging Using Transient Electrode Perturbation: Phantom and ex vivo Validation. IEEE Transactions on Medical Imaging, 2011, 30, 666-678.	8.9	32
53	The relationship between carotid artery plaque stability and white matter ischemic injury. NeuroImage: Clinical, 2015, 9, 216-222.	2.7	32
54	Second Prize: Elastographic Measurements of in-Vivo Radiofrequency Ablation Lesions of the Kidney. Journal of Endourology, 2006, 20, 959-964.	2.1	31

#	Article	IF	CITATIONS
55	In Vitro Uterine Strain Imaging. Journal of Ultrasound in Medicine, 2007, 26, 899-908.	1.7	30
56	Characterizing the compression-dependent viscoelastic properties of human hepatic pathologies using dynamic compression testing. Physics in Medicine and Biology, 2012, 57, 2273-2286.	3.0	30
57	Ultrasound frame rate requirements for cardiac elastography: Experimental and in vivo results. Ultrasonics, 2009, 49, 98-111.	3.9	29
58	Tissue mimicking materials for the detection of prostate cancer using shear wave elastography: A validation study. Medical Physics, 2013, 40, 022903.	3.0	29
59	Multilevel hybrid 2D strain imaging algorithm for ultrasound sector/phased arrays. Medical Physics, 2009, 36, 2098-2106.	3.0	28
60	Ultrasound-based relative elastic modulus imaging for visualizing thermal ablation zones in a porcine model. Physics in Medicine and Biology, 2010, 55, 2281-2306.	3.0	28
61	Impaired cognitive function in patients with atherosclerotic carotid stenosis and correlation with ultrasound strain measurements. Journal of the Neurological Sciences, 2012, 322, 20-24.	0.6	28
62	Segmentation of elastographic images using a coarse-to-fine active contour model. Ultrasound in Medicine and Biology, 2006, 32, 397-408.	1.5	27
63	Visualizing <i>ex vivo</i> radiofrequency and microwave ablation zones using electrode vibration elastography. Medical Physics, 2012, 39, 6692-6700.	3.0	27
64	An Approach to Unbiased Subsample Interpolation for Motion Tracking. Ultrasonic Imaging, 2013, 35, 76-89.	2.6	27
65	Deep Learning for Carotid Plaque Segmentation using a Dilated U-Net Architecture. Ultrasonic Imaging, 2020, 42, 221-230.	2.6	27
66	The Preservation of Cognition 1 Year After Carotid Endarterectomy in Patients With Prior Cognitive Decline. Neurosurgery, 2018, 82, 322-328.	1.1	25
67	Ultrasound Attenuation Imaging Using Compound Acquisition and Processing. Ultrasonic Imaging, 2003, 25, 245-261.	2.6	24
68	Relationship Between Ultrasonic Attenuation, Size and Axial Strain Parameters for Ex Vivo Atherosclerotic Carotid Plaque. Ultrasound in Medicine and Biology, 2008, 34, 1666-1677.	1.5	24
69	Dynamic and quasi-static mechanical testing for characterization of the viscoelastic properties of human uterine tissue. Journal of Biomechanics, 2015, 48, 1730-1736.	2.1	24
70	Adaptive Spectral Strain Estimators for Elastography. Ultrasonic Imaging, 2004, 26, 131-149.	2.6	23
71	Numerical Study of Microwave Scattering in Breast Tissue via Coupled Dielectric and Elastic Contrasts. IEEE Antennas and Wireless Propagation Letters, 2008, 7, 247-250.	4.0	23
72	GPU Accelerated Multilevel Lagrangian Carotid Strain Imaging. IEEE Transactions on Ultrasonics, Ferroelectrics, and Frequency Control, 2018, 65, 1370-1379.	3.0	23

#	Article	IF	CITATIONS
73	Real-Time in Vivo Photoacoustic Imaging in the Assessment of Myocardial Dynamics in Murine Model of Myocardial Ischemia. Ultrasound in Medicine and Biology, 2018, 44, 2155-2164.	1.5	23
74	Performance evaluation of the spectral centroid downshift method for attenuation estimation. IEEE Transactions on Ultrasonics, Ferroelectrics, and Frequency Control, 2015, 62, 871-880.	3.0	22
75	Post-Procedure Evaluation of Microwave Ablations of Hepatocellular Carcinomas Using Electrode Displacement Elastography. Ultrasound in Medicine and Biology, 2016, 42, 2893-2902.	1.5	22
76	In vivo attenuation and equivalent scatterer size parameters for atherosclerotic carotid plaque: Preliminary results. Ultrasonics, 2009, 49, 779-785.	3.9	21
77	Dynamic frame selection for <i>in vivo</i> ultrasound temperature estimation during radiofrequency ablation. Physics in Medicine and Biology, 2010, 55, 4735-4753.	3.0	21
78	Quantifying Local Stiffness Variations in Radiofrequency Ablations With Dynamic Indentation. IEEE Transactions on Biomedical Engineering, 2012, 59, 728-735.	4.2	21
79	Contrast-transfer improvement for electrode displacement elastography. Physics in Medicine and Biology, 2006, 51, 6403-6418.	3.0	20
80	Shear strain imaging using shear deformations. Medical Physics, 2008, 35, 412-423.	3.0	20
81	Radiofrequency electrode vibration-induced shear wave imaging for tissue modulus estimation: A simulation study. Journal of the Acoustical Society of America, 2010, 128, 1582-1585.	1.1	20
82	Optimum Diffraction-Corrected Frequency-Shift Estimator of the Ultrasonic Attenuation Coefficient. IEEE Transactions on Ultrasonics, Ferroelectrics, and Frequency Control, 2016, 63, 691-702.	3.0	20
83	Monitoring Microwave Ablation of ExÂVivo Bovine Liver Using Ultrasonic Attenuation Imaging. Ultrasound in Medicine and Biology, 2017, 43, 1441-1451.	1.5	20
84	Spectral estimators in elastography. Ultrasonics, 2000, 38, 412-416.	3.9	19
85	Elastographic versus x-ray CT imaging of radio frequency ablation coagulations: Anin vitrostudy. Medical Physics, 2004, 31, 1322-1332.	3.0	19
86	Correlation of RF signals during angular compounding. IEEE Transactions on Ultrasonics, Ferroelectrics, and Frequency Control, 2005, 52, 961-970.	3.0	19
87	Influence of Ultrasound System and Gain on Grayscale Median Values. Journal of Ultrasound in Medicine, 2019, 38, 307-319.	1.7	19
88	Mean scatterer spacing estimation using multi-taper coherence. IEEE Transactions on Ultrasonics, Ferroelectrics, and Frequency Control, 2013, 60, 1061-1073.	3.0	18
89	Improved Correlation of Strain Indices with Cognitive Dysfunction with Inclusion of Adventitial Layer with Carotid Plaque. Ultrasonic Imaging, 2016, 38, 194-208.	2.6	18
90	Locally optimized correlation-guided Bayesian adaptive regularization for ultrasound strain imaging. Physics in Medicine and Biology, 2020, 65, 065008.	3.0	18

#	Article	IF	CITATIONS
91	Evaluation of acoustic wave propagation velocities in the ocular lens and vitreous tissues of pigs, dogs, and rabbits. American Journal of Veterinary Research, 2006, 67, 288-295.	0.6	17
92	In Vivo Classification of Breast Masses Using Features Derived From Axial-Strain and Axial-Shear Images. Ultrasonic Imaging, 2012, 34, 222-236.	2.6	17
93	Lagrangian displacement tracking using a polar grid between endocardial and epicardial contours for cardiac strain imaging. Medical Physics, 2012, 39, 1779-1792.	3.0	17
94	Scatterer Number Density Considerations in Reference Phantom-Based Attenuation Estimation. Ultrasound in Medicine and Biology, 2014, 40, 1680-1696.	1.5	17
95	Three-Dimensional Sheaf of Ultrasound Planes Reconstruction (SOUPR) of Ablated Volumes. IEEE Transactions on Medical Imaging, 2014, 33, 1677-1688.	8.9	17
96	Hierarchical Motion Estimation With Bayesian Regularization in Cardiac Elastography: Simulation and \$In~ Vivo\$ Validation. IEEE Transactions on Ultrasonics, Ferroelectrics, and Frequency Control, 2019, 66, 1708-1722.	3.0	17
97	Finite element analysis of tissue deformation with a radiofrequency ablation electrode for strain imaging. IEEE Transactions on Ultrasonics, Ferroelectrics, and Frequency Control, 2007, 54, 281-289.	3.0	16
98	Ultrasonic Noninvasive Temperature Estimation Using Echoshift Gradient Maps: Simulation Results. Ultrasonic Imaging, 2005, 27, 166-180.	2.6	15
99	Compression-Dependent Viscoelastic Behavior of Human Cervix Tissue. Ultrasonic Imaging, 2010, 32, 214-228.	2.6	15
100	Noise reduction using spatial-angular compounding for elastography. IEEE Transactions on Ultrasonics, Ferroelectrics, and Frequency Control, 2004, 51, 510-20.	3.0	15
101	Threeâ€dimensional canine heart model for cardiac elastography. Medical Physics, 2010, 37, 5876-5886.	3.0	14
102	Ex vivo ultrasound attenuation coefficient for human cervical and uterine tissue from 5 to 10MHz. Ultrasonics, 2011, 51, 467-471.	3.9	14
103	Improved parametric imaging of scatterer size estimates using angular compounding. IEEE Transactions on Ultrasonics, Ferroelectrics, and Frequency Control, 2004, 51, 708-15.	3.0	14
104	Correlation analysis of the beam angle dependence for elastography. Journal of the Acoustical Society of America, 2006, 119, 4093-4101.	1.1	13
105	Anthropomorphic Phantoms for Assessment of Strain Imaging Methods Involving Saline-Infused Sonohysterography. Ultrasound in Medicine and Biology, 2008, 34, 1622-1637.	1.5	13
106	Estimation of the Optimal Maximum Beam Angle and Angular Increment for Normal and Shear Strain Estimation. IEEE Transactions on Biomedical Engineering, 2009, 56, 760-769.	4.2	13
107	Delineation of Post-Procedure Ablation Regions with Electrode Displacement Elastography with a Comparison to Acoustic Radiation Force Impulse Imaging. Ultrasound in Medicine and Biology, 2017, 43, 1953-1962.	1.5	13
108	Transcranial Doppler and Microemboli Detection: Relationships to Symptomatic Status and Histopathology Findings. Ultrasound in Medicine and Biology, 2017, 43, 1861-1867.	1.5	13

#	Article	IF	CITATIONS
109	Spatiotemporal Coherence Weighting for <i>In Vivo</i> Cardiac Photoacoustic Image Beamformation. IEEE Transactions on Ultrasonics, Ferroelectrics, and Frequency Control, 2021, 68, 586-598.	3.0	13
110	Correlation of ultrasonic scatterer size estimates for the statistical analysis and optimization of angular compounding. Journal of the Acoustical Society of America, 2004, 116, 1832-1841.	1.1	12
111	Correlation analysis of three-dimensional strain imaging using ultrasound two-dimensional array transducers. Journal of the Acoustical Society of America, 2008, 124, 1858-1865.	1.1	12
112	Theoretical and phantom based investigation of the impact of sound speed and backscatter variations on attenuation slope estimation. Ultrasonics, 2011, 51, 758-767.	3.9	12
113	Relative Elastic Modulus Imaging Using Sector Ultrasound Data for Abdominal Applications: An Evaluation of Strategies and Feasibility. IEEE Transactions on Ultrasonics, Ferroelectrics, and Frequency Control, 2016, 63, 1432-1440.	3.0	12
114	Segmental Analysis of Cardiac Short-Axis Views Using Lagrangian Radial and Circumferential Strain. Ultrasonic Imaging, 2016, 38, 363-383.	2.6	12
115	Comparison of Displacement Tracking Algorithms for in Vivo Electrode Displacement Elastography. Ultrasound in Medicine and Biology, 2019, 45, 218-232.	1.5	12
116	Marrow-Derived Autologous Stromal Cells for the Restoration of Salivary Hypofunction (MARSH): Study protocol for a phase 1 dose-escalation trial of patients with xerostomia after radiation therapy for head and neck cancer. Cytotherapy, 2022, 24, 534-543.	0.7	12
117	A general solution for catheter position effects for strain estimation in intravascular elastography. Ultrasound in Medicine and Biology, 2005, 31, 1509-1526.	1.5	11
118	Evaluation of the impact of backscatter intensity variations on ultrasound attenuation estimation. Medical Physics, 2013, 40, 082904.	3.0	11
119	Correlation Analysis for Angular Compounding in Strain Imaging. IEEE Transactions on Ultrasonics, Ferroelectrics, and Frequency Control, 2007, 54, 1903-1907.	3.0	10
120	Displacement and strain estimation for evaluation of arterial wall stiffness using a familial hypercholesterolemia swine model of atherosclerosis. Medical Physics, 2012, 39, 4483-4492.	3.0	10
121	Mean Scatterer Spacing Estimation in Normal and Thermally Coagulated Ex Vivo Bovine Liver. Ultrasonic Imaging, 2014, 36, 79-97.	2.6	10
122	Phase aberration effects in elastography. Ultrasound in Medicine and Biology, 2001, 27, 819-827.	1.5	9
123	Absolute backscatter coefficient estimates of tissue-mimicking phantoms in the 5–50 MHz frequency range. Journal of the Acoustical Society of America, 2011, 130, 737-743.	1.1	9
124	Analysis of shear strain imaging for classifying breast masses: Finite element and phantom results. Medical Physics, 2011, 38, 6119-6127.	3.0	9
125	Normal and shear strain imaging using 2D deformation tracking on beam steered linear array datasets. Medical Physics, 2013, 40, 012902.	3.0	9
126	Slope estimation in noisy piecewise linear functions. Signal Processing, 2015, 108, 576-588.	3.7	9

#	Article	IF	CITATIONS
127	Dictionary Representations for Electrode Displacement Elastography. IEEE Transactions on Ultrasonics, Ferroelectrics, and Frequency Control, 2018, 65, 2381-2389.	3.0	9
128	A Method for Experimental Characterization of the Noise Performance of Elastographic Systems. Ultrasonic Imaging, 1999, 21, 17-30.	2.6	8
129	Elastography. Comptes Rendus Physique, 2001, 2, 1193-1212.	0.1	8
130	Lower Bound on Estimation Variance of the Ultrasonic Attenuation Coefficient Using the Spectral-Difference Reference-phantom Method. Ultrasonic Imaging, 2017, 39, 151-171.	2.6	8
131	In vivo carotid strain imaging using principal strains in longitudinal view. Biomedical Physics and Engineering Express, 2019, 5, 035030.	1.2	8
132	Ultrasonic Attenuation Estimation in Small Plaque Samples Using a Power Difference Method. Ultrasonic Imaging, 2007, 29, 15-30.	2.6	7
133	Principal component analysis of shear strain effects. Ultrasonics, 2009, 49, 472-483.	3.9	7
134	Improving thermal ablation delineation with electrode vibration elastography using a bidirectional wave propagation assumption. IEEE Transactions on Ultrasonics, Ferroelectrics, and Frequency Control, 2012, 59, 168-173.	3.0	7
135	Signal to noise ratio comparisons for ultrasound attenuation slope estimation algorithms. Medical Physics, 2014, 41, 032902.	3.0	7
136	Twoâ€dimensional ultrasound omputed tomography image registration for monitoring percutaneous hepatic intervention. Medical Physics, 2019, 46, 2600-2609.	3.0	7
137	Subaperture Processing-Based Adaptive Beamforming for Photoacoustic Imaging. IEEE Transactions on Ultrasonics, Ferroelectrics, and Frequency Control, 2021, 68, 2336-2350.	3.0	7
138	Estimation of ultrasound attenuation from broadband echo-signals using bandpass filtering. IEEE Transactions on Ultrasonics, Ferroelectrics, and Frequency Control, 2008, 55, 1153-1159.	3.0	6
139	Noise analysis and improvement of displacement vector estimation from angular displacements. Medical Physics, 2008, 35, 2007-2017.	3.0	6
140	A Novel Saline Infusion Sonohysterography-Based Strain Imaging Approach for Evaluation of Uterine Abnormalities In Vivo. Journal of Ultrasound in Medicine, 2012, 31, 609-615.	1.7	6
141	Ultrasonic tracking of shear waves using a particle filter. Medical Physics, 2015, 42, 6711-6724.	3.0	6
142	Comparison of three dimensional strain volume reconstructions using SOUPR and wobbler based acquisitions: A phantom study. Medical Physics, 2016, 43, 1615-1626.	3.0	6
143	Enhancement of in vivo cardiac photoacoustic signal specificity using spatiotemporal singular value decomposition. Journal of Biomedical Optics, 2021, 26, .	2.6	6
144	Spatiotemporal Bayesian Regularization for Cardiac Strain Imaging: Simulation and <i>In Vivo</i> Results. IEEE Open Journal of Ultrasonics, Ferroelectrics, and Frequency Control, 2021, 1, 21-36.	1.4	6

#	Article	IF	CITATIONS
145	Simulation of ultrasound two-dimensional array transducers using a frequency domain model. Medical Physics, 2008, 35, 3162-3169.	3.0	5
146	Efficient 3-D Reconstruction in Ultrasound Elastography via a Sparse Iteration Based on Markov Random Fields. IEEE Transactions on Ultrasonics, Ferroelectrics, and Frequency Control, 2017, 64, 491-499.	3.0	5
147	Physiological Motion Reduction Using Lagrangian Tracking for Electrode Displacement Elastography. Ultrasound in Medicine and Biology, 2020, 46, 766-781.	1.5	5
148	Ultrasonic attenuation imaging using spectral cross-correlation and the reference phantom method. , 2011, , .		4
149	Lagrangian carotid strain imaging indices normalized to blood pressure for vulnerable plaque. Journal of Clinical Ultrasound, 2019, 47, 477-485.	0.8	4
150	Improving Ultrasound Lateral Strain Estimation Accuracy using Log Compression of Regularized Correlation Function. , 2020, 2020, 2031-2034.		4
151	Attenuation Coefficient Parameter Computations for Tissue Composition Assessment of Carotid Atherosclerotic Plaque in Vivo. Ultrasound in Medicine and Biology, 2020, 46, 1513-1532.	1.5	4
152	Murine cardiac fibrosis localization using adaptive Bayesian cardiac strain imaging in vivo. Scientific Reports, 2022, 12, .	3.3	4
153	Experimental corroboration of the nonstationary strain estimation errors in elastography. Ultrasound in Medicine and Biology, 2001, 27, 1677-1682.	1.5	3
154	Carotid plaque characterization with histology and quantitative ultrasound. , 2014, , .		3
155	Analysis of 2-D Ultrasound Cardiac Strain Imaging Using Joint Probability Density Functions. Ultrasound in Medicine and Biology, 2014, 40, 1118-1132.	1.5	3
156	Carotid Plaque Strain Indices Were Correlated With Cognitive Performance in a Cohort With Advanced Atherosclerosis, and Traditional Doppler Measures Showed no Association. Journal of Ultrasound in Medicine, 2020, 39, 2033-2042.	1.7	3
157	Cardiac Strain Imaging with Dynamically Skipped Frames: A Simulation Study. , 2020, , .		3
158	Elastic modulus imaging (EMI) for visualizing thermal ablation zone: Initial experience in a porcine model. , 2009, , .		2
159	In vivo ultrasound electrode displacement strain imaging. , 2009, , .		2
160	Stochastic piecewise linear function fitting with application to ultrasound shear wave imaging. , 2014, 2014, 2861-4.		2
161	Comparison of cardiac displacements in a murine model of myocardial ischemia using cardiac elastography and Speckle Tracking Echocardiography. , 2017, , .		2
162	Normalization of carotid plaque based strain indices using blood pressure measurements. , 2017, , .		2

10

Tomy Varghese

#	Article	IF	CITATIONS
163	In-vivo quantitative ultrasound evaluation of carotid plaque. , 2017, , .		2
164	Singular value decomposition processing for in vivo cardiac photoacoustic imaging. , 2021, , .		2
165	Carotid Strain Imaging with a Locally Optimized Adaptive Bayesian Regularized Motion Tracking Algorithm. , 2020, , .		2
166	Photoacoustic Delay-and-Sum Beamforming with Spatiotemporal Coherence Factor. , 2020, , .		2
167	Nonlinear mechanical behavior of cervical tissue with increasing pre-compression. , 2009, , .		1
168	Coherence of ultrasound radiofrequency echoes from the liver estimated using multi-taper calculation. , 2013, 2013, 724-727.		1
169	A comparison of model based and direct optimization based filtering algorithms for shearwave velocity reconstruction for electrode vibration elastography. , 2013, 2013, 760-763.		1
170	Fast multilevel Lagrangian carotid strain imaging with GPU computing. , 2017, , .		1
171	Study of the Relationship Between Ultrasound Strain Indices and Cognitive Decline for Vulnerable Carotid Plaque. , 2020, 2020, 2088-2091.		1
172	Interstitial diffuse optical probe with spectral fitting to measure dynamic tumor hypoxia. Biomedical Physics and Engineering Express, 2020, 6, 015039.	1.2	1
173	Ultrasound strain imaging using spatiotemporal Bayesian regularized multi-level block matching method. , 2021, , .		1
174	Differential Imaging of Liver Tumors before and after Microwave Ablation with Electrode Displacement Elastography. Ultrasound in Medicine and Biology, 2021, 47, 2138-2156.	1.5	1
175	Abstract WMP47: Traditional Doppler Measures Do Not predict Cognition in a Cohort With Advanced Atherosclerosis. Stroke, 2019, 50, .	2.0	1
176	In vivo Apical Infarct Localization using Adaptive Bayesian Cardiac Strain Imaging. , 2021, , .		1
177	Coupled Sub-aperture and Spatiotemporal Singular Value Decomposition Processing for Cardiac Photoacoustic Imaging In Vivo. , 2021, , .		1
178	Bayesian Regularized Strain Imaging for Assessment of Murine Cardiac Function In vivo. , 2021, 2021, 2883-2886.		1
179	Improving Minimum Variance Beamforming with Sub-Aperture Processing for Photoacoustic Imaging. , 2021, 2021, 2879-2882.		1
180	Axial shear strain imaging for breast mass differentiation. , 2009, , .		0

180 Axial shear strain imaging for breast mass differentiation. , 2009, , .

#	Article	IF	CITATIONS
181	Shear wave velocity imaging using transient electrode perturbation: A phantom study. , 2010, , .		0
182	Ultrasound saline infused sonohysterography based in-vivo strain imaging for the evaluation of uterine abnormalities. , 2010, , .		0
183	Analysis of shear strain imaging for classifying breast masses. , 2010, , .		0
184	Quantifying local stiffness variations in radiofrequency ablations with dynamic indentation. , 2011, , .		0
185	Improving thermal ablation delineation with electrode vibration elastography using a bidirectional wave propagation assumption. , 2011, , .		0
186	Feature based analysis of axial-shear strain imaging for breast mass classification. , 2011, , .		0
187	C-plane reconstructions from sheaf acquisition for ultrasound electrode vibration elastography. , 2014, 2014, 1826-1829.		0
188	Three dimensional shear wave elastographic reconstruction of ablations. , 2014, 2014, 2857-60.		0
189	The effect of low scatterer number density on ultrasound attenuation estimation. , 2014, , .		Ο
190	Alterations in ultrasound scattering following thermal ablation in ex vivo bovine liver. , 2014, 2014, 1904-1907.		0
191	Comparison of cardiac displacements in a murine model of myocardial ischemia using Cardiac Elastography and speckle tracking echocardiography. , 2017, , .		0
192	Normalization of carotid plaque based strain indices using blood pressure measurements. , 2017, , .		0
193	Improved delineation rate of thermally ablated liver tumors with electrode displacement elastography compared to commercial acoustic radiation force impulse imaging. , 2017, , .		0
194	Fast multilevel Lagrangian carotid strain imaging with GPU computing. , 2017, , .		0
195	Comparison study of displacement estimation methods for microwave ablation procedures using electrode displacement elastography. , 2017, , .		0
196	3D reconstruction of ablations in shear wave elastography using the matern kernel. , 2017, , .		0
197	Update on carotid plaque instability quantification using strain indices from multiple regions of interest in carotid plaque. , 2017, , .		0
198	Update on carotid plaque instability quantification using strain indices from multiple regions of interest in carotid plaque. , 2017, , .		0

#	Article	IF	CITATIONS
199	Delineation of microwave ablated hepatocellular carcinoma tumor regions using electrode displacement elastography. , 2017, , .		0
200	3D reconstruction of ablations in shear wave elastography using the mat $ ilde{A}$ ©rn kernel. , 2017, , .		0
201	Notice of Removal: In-vivo quantitative ultrasound evaluation of carotid plaque. , 2017, , .		0
202	Comparison study of displacement estimation methods for microwave ablation procedures using electrode displacement elastography. , 2017, , .		0
203	In Reply: The Preservation of Cognition 1 Year After Carotid Endarterectomy in Patients With Prior Cognitive Decline. Neurosurgery, 2018, 83, E181-E181.	1.1	0
204	A kernel smoothing algorithm for ablation visualization in ultrasound elastography. Ultrasonics, 2019, 96, 267-275.	3.9	0
205	Lateral and shear strain imaging for ultrasound elastography. , 2020, , 167-183.		0
206	Adaptation of Dictionary Learning for Electrode Displacement Elastography*. , 2020, 2020, 2023-2026.		0
207	Electrode displacement elastography for differentiating metastatic liver cancer microwave ablation procedures. , 2021, , .		0
208	Lagrangian Deformation Tracking for Microwave Ablation Zones. , 2021, , .		0
209	Attenuation Coefficient Parameter Estimations to Characterize Ex Vivo Carotid Plaque. , 2020, , .		Ο